SUPPORTING INFORMATION

Multicore assemblies potentiate magnetic properties of biomagnetic nanoparticles

Taejong Yoon[1,2#], Hakho Lee[1#*], Huilin Shao[1], Scott A. Hilderbrand[1], and Ralph Weissleder[1,3*]

[1] Center for Systems Biology, Massachusetts General Hospital, 185 Cambridge St, Boston, MA 02114
[2] Department of Applied Bioscience, CHA University, Seoul 135-081, Republic of Korea
[3] Department of Systems Biology, Harvard Medical School, Boston, MA 02115

[#] These authors contributed equally.

SUPPORTING FIGURES AND TABLE

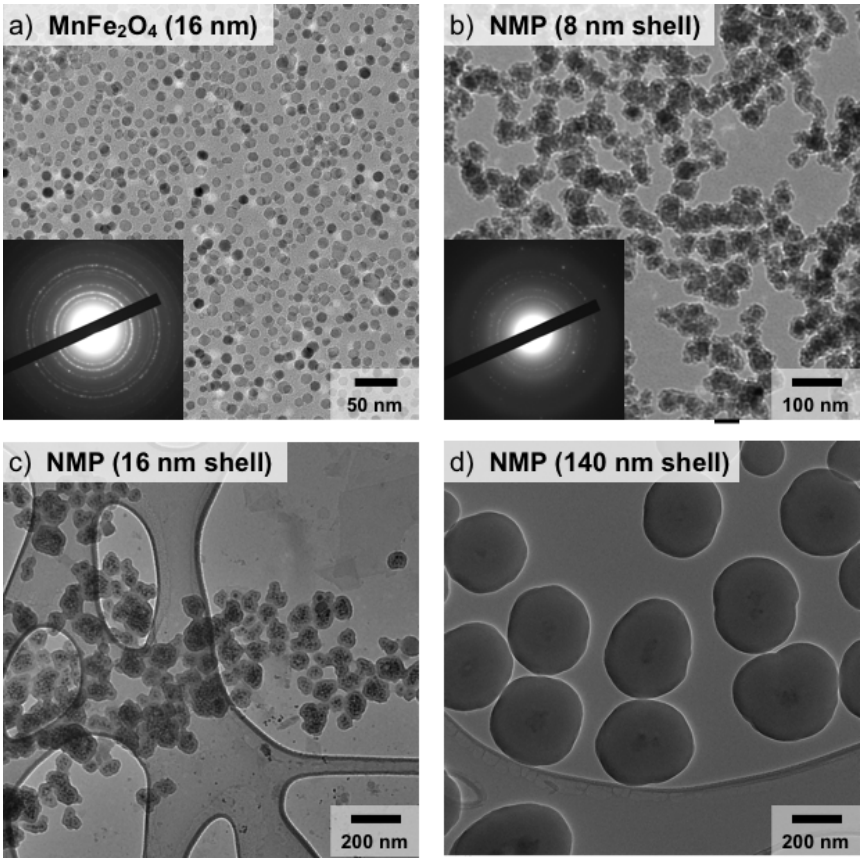

Figure S1. Transmission electron microscope (TEM) images of manganese magnetic nanoparticles (Mn-MNPs) and nano-magnetic pomegranate particles (NMPs) at low magnification. (a) TEM image showing the 16 nm $MnFe_2O_4$ MNPs (Mn-MNPs) that were used as the magnetic core for NMPs. Electron diffraction (ED) patterns (inset) verified the high crystallinity of the particles. (**b, c & d)** NMPs with varying shell thickness. ED patterns (inset in b) confirmed that the Mn-MNP cores maintained their crystallinity. Note that as NMPs dispersed in water, they tended to aggregate during deposition and drying on the TEM grids.

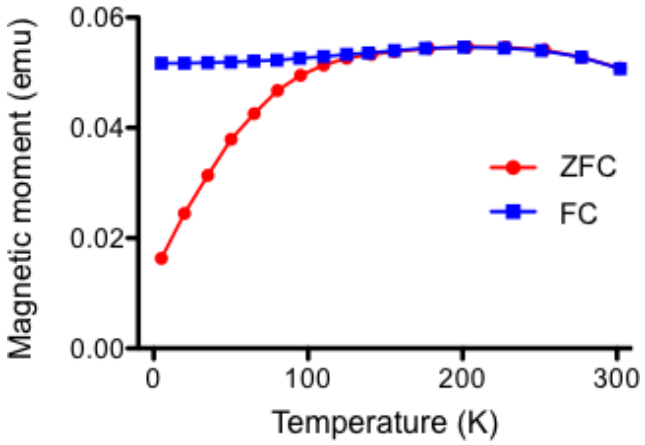

Figure S2. Temperature-dependent magnetization of NMPs. By measuring the zero-field cooling (ZFC) and field cooling (FC) magnetization of NMPs (overall diameter 87 nm), the blocking temperature could be estimated at ~200 K. NMPs were thus superparamagnetic at room temperature.

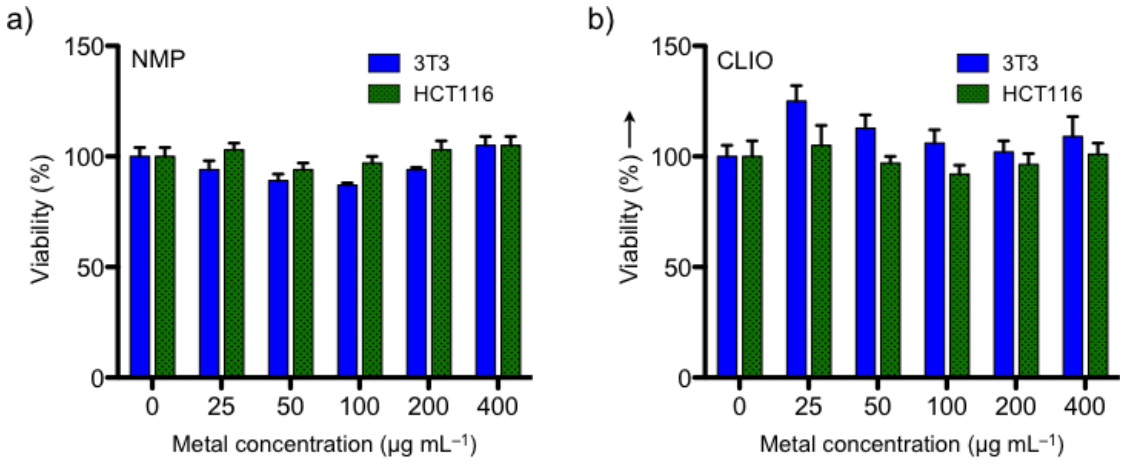

Figure S3. Cytotoxicity of NMPs. (a) Normal (3T3 fibroblast) and cancer (HCT116) cells were incubated for 24 hours in the presence of varying amounts of NMPs. Cellular viability was then measured using a 3-(4,5-dimethylthiazol-2-yl)-2,5-diphenyltetrazolium (MTT) bromide assay. No acute cytotoxic effects were observed, even at a high metal dose of 400 µg/mL. The assay thus verified the biocompatibility of the NMPs. **(b)** As a positive control, a similar viability test was performed using CLIO (cross-linked iron oxide), and the results showed comparable trends.

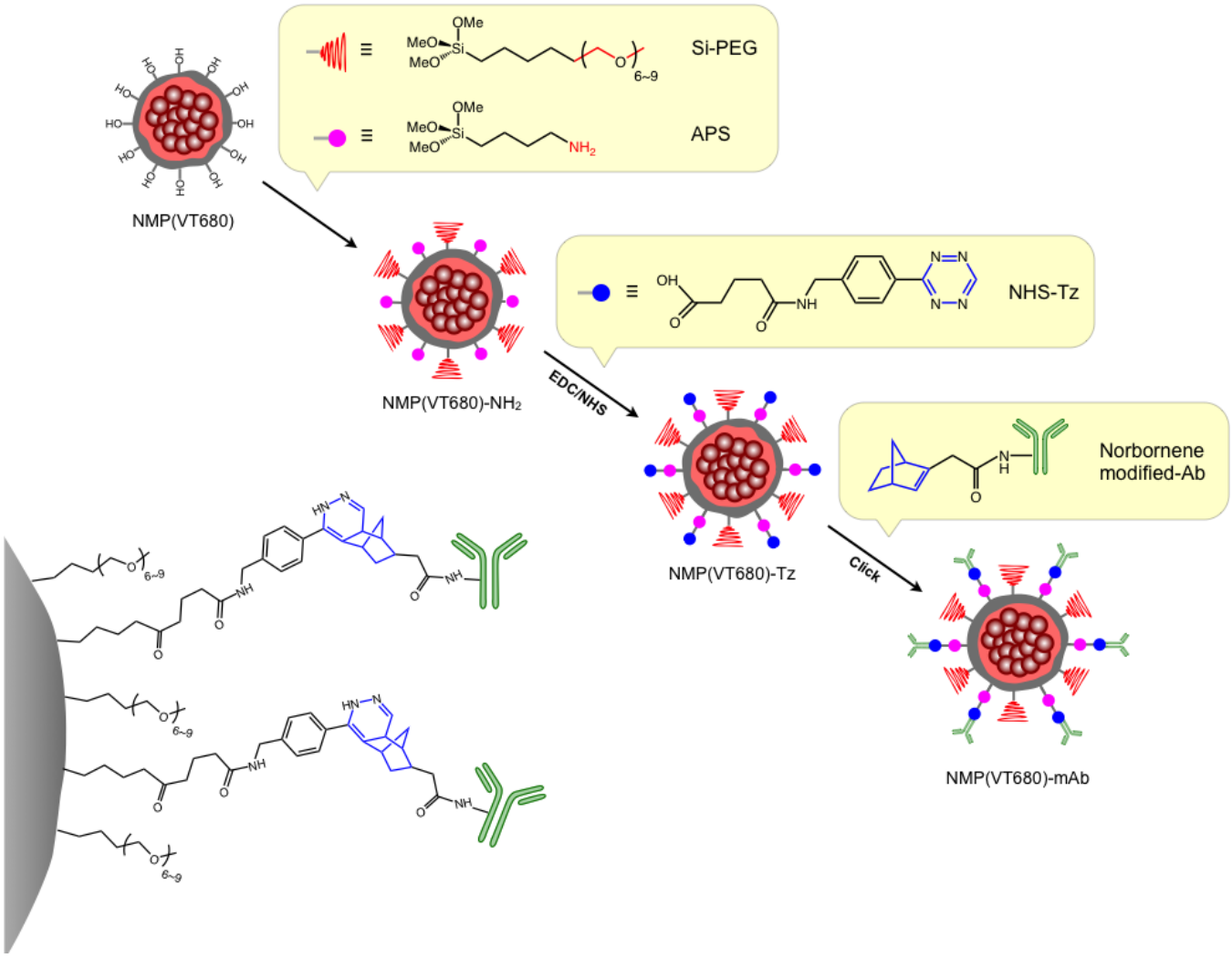

Figure S4. Bioorthogonal conjugation of NMPs. To conjugate targeting molecules (e.g., antibodies) onto NMPs, we utilized the Diels-Alder cycloaddition between tetrazine (Tz) and norbornene. As-prepared NMPs were treated with 2-[methoxy(polyethyleneoxy)propyl]trimethoxysilane (Si-PEG) and 3-aminopropyltriethyoxysilane (APS) to enhance their water solubility and to provide primary amine groups. Tz was then attached to the NMPs via an amide bond formed through ethyl(dimethylaminopropyl) carbodiimide/N-Hydroxysuccinimide (EDC/ NHS) chemistry. Antibodies were initially modified with norbornene before being mixed with Tz-NMPs. The reaction was fast (< 1 hour) and resulted in stable immobilization of antibodies on the particle surface.

a)

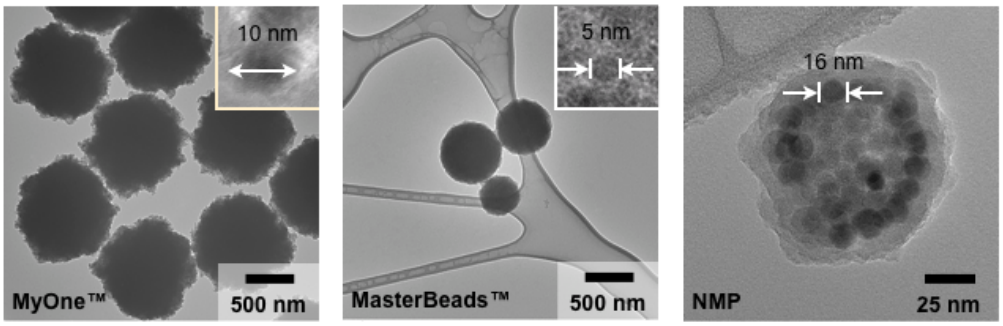

	MyOne™	MasterBeads™	NMP
Total size (nm)	1000	500	80
Magnetic core, size	$\gamma Fe_2O_3/Fe_3O_4$ (10 nm)	$\gamma Fe_2O_3/Fe_3O_4$ (5 nm)	$MnFe_2O_4$ (16 nm)
Surface coating	Polystyrene	SiO_2	SiO_2
Dispersibility in H_2O	– (Heterogeneous)	+ (Heterogeneous)	+++ (Homogeneous)
Sedimentation	Fast	Slow	None

b)

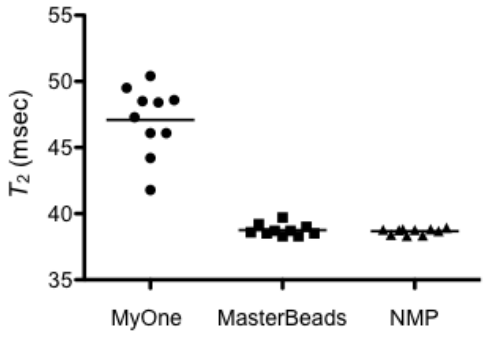

c)

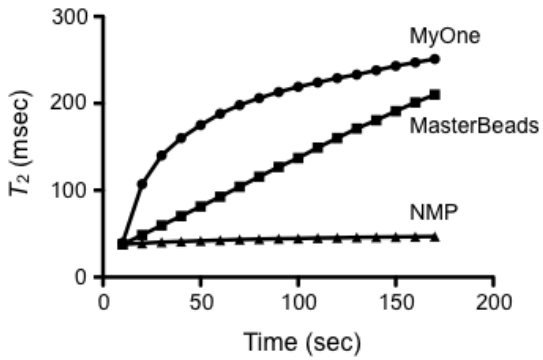

Figure S5. Comparison of NMPs with other types of multicore magnetic nanoparticles (MNPs). (a) NMPs were compared with other commercially available representative multicore MNPs. While MyOne (Invitrogen) and MasterBeads (Adamtech) contain greater magnetic material due to their large size, their core MNPs are smaller and magnetically weaker than NMP core particles (Mn-MNPs). Since transverse relaxivity (r_2) is determined by the magnetization of the core particles, this would lead MyOne and Masterbeads to have lower r_2 values (per metal concentration) in the static dephasing regime,. **(b)** The reproducibility of T_2 measurements was examined by performing repeat measurements on the same samples. MyOne particles showed large T_2 variations due to the heterogeneous dispersion of the particles in water. **(c)** When T_2 values were monitored over time, the T_2 drift was more pronounced with MyOne and MasterBeads than with NMPs. This drift was caused by the particles sedimenting in solution and thus becoming invisible to the NMR detector. In contrast, due to their excellent dispersion in water, NMPs maintained stable T_2 values over time.

MNPs		Magnetic core diameter (nm)	Shell thickness (nm)	Whole size (nm)	Relaxivity (s^{-1} mM^{-1} [metal])		Relaxivity ($\times10^{-15}$ s^{-1} L^{-1})	
					r_1 (longitudinal)	r_2 (transverse)	r_1 (longitudinal)	r_2 (transverse)
Single core	CLIO	7	15	37	20	50	0.02	0.05
	$MnFe_2O_4$	10	2	14	16	218	0.6	8
	$MnFe_2O_4$	12	2	16	35	382	2.1	23
	$MnFe_2O_4$	16	2	20	44	414	6.4	60
Multicore	NMP	68	9	86	3.9	695	32.1	5.7×10^3
		68	12	92	2.8	687	23.1	5.6×10^3
		68	16	100	2.2	624	18.1	5.1×10^3
		70	140	350	0.8	558	7.2	5.0×10^3

Table S1. Comparison of the physical properties of single core MNPs with those of NMPs.

SUPPORTING METHODS

Iron (III) acetylacetonate (99.9 %, $Fe(acac)_3$), Iron (II) acetylacetonate (99.95 %, $Fe(acac)_2$), 1,2-Hexadecandiol (90 %), Oleic acid (99 %, OA), Oleylamine (70 %, OY), Cobalt (II) acetylacetonate $Co(acac)_2$ (97 %), Manganese (II) acetylacetonate $Mn(acac)_2$, Oleylamine (70 %), 1-Octadecene (95 %, ODE), Chloroform (99 %), 2,3-Dimercaptosuccinic acid (98 %, DMSA), Triethylamine (99 %), Dimethyl sulfoxide (99.9 %, DMSO), poly-vinylpyrrolidone solution (PVP, Mr 55,000 Da), Tetraethyl orthosilicate (TEOS, 99.999 %) 2[methoxy(polyethyleneoxy)propyl]trimethoxysilane (Si-PEG), 3-aminopropyltriethyoxysilane (APS), N-(3-Dimethylaminopropyl)-N'-ethylcarbodiimide hydrochloride (EDC), N-Hydroxysulfosuccinimide sodium salt (Sulfo-NHS, 98.5 %) and 3-(*p*-benzylamino)-1,2,4,5-tetrazine (tetrazine) were purchased (Sigma-Aldrich or Gelest) and used without further modification. Isopropanol (99.5 %), hexane (98.5 %), ethanol (99.5 %) and sodium bicarbonate ($NaHCO_3$) were purchased (Fisher Scientific) and used without further purification.

Synthesis of magnetic cores (16 nm Mn-MNPs)[1]: 10 nm Mn-MNPs were initially synthesized as seeds for subsequent particle growth. $Fe(acac)_3$ (4 mmoL, 1.4 g), $Mn(acac)_2$ (2 mmoL, 0.5 g), 1,2-hexadecanediol (10 mmoL, 2.9 g), OA (6 mmoL, 1.9 mL), OY (6 mmoL, 2.8 mL) and ODE (20 mL) were mixed by stirring under N_2 flow for 1 hour. The mixture was heated and kept at 200 °C for 2 hours. The temperature was then quickly raised to 280 °C to initiate particle formation. After reflux, the mixture was cooled to room temperature and isopropanol (4 mL) was added. Mn-MNPs were collected by centrifugation (1811 × g, 15 minutes) and the precipitates were redispersed in hexane. To make larger Mn-MNPs, the 10 nm Mn-MNPs (100 mg) were dissolved in hexane (10 mL) together with the same amounts of metal acetylacetonates, 1,2-hexadecanediol, OA, OY and ODE, as described above. Under N_2 flow, the mixture was heated and kept at 100 °C for 1 hour. The temperature was then elevated to 200 °C and maintained for 2 hours. Finally, the mixture was heated again to 300 °C and refluxed for 2 hours before being cooled down to room temperature. The particles (12 nm Mn-MNPs) were collected using the same washing and isolation procedure as that described above. 16 nm Mn-MNPs were subsequently prepared using the 12 nm particles as seeds. The morphology and structure of Mn-MNPs were characterized using a transmission electron microscope (TEM; JEOL 2100, JOEL USA) and an X-ray powder diffractometer (XRD; RU300, Rigaku), respectively. The composition of Mn-MNPs, analyzed by an inductively-coupled plasma atomic emission spectrometer (ICP-AES; Activa-S, HORIBA Jobin Yvon), was close to that of the chemical formula ([Mn]:[Fe] = 1:2). The magnetic properties were measured by a superconducting quantum interference device (SQUID) magnetometer and a vibrating sample magnetometer.

Synthesis and characterization of NMPs: The 16 nm Mn-MNPs (prepared above) were dissolved in chloroform (10 mL) along with 50 µL triethylamine. DMSA (50 mg in 10 mL DMSO) was injected, and the mixture was shaken for 6 hours at 40 °C until heterogeneous. Particles were then collected via centrifugation (1811 × g; 10 minutes). The precipitate was carefully washed with ethanol to remove excess DMSA, and dispersed in 10 mL ethanol using a homogenizer. DMSA (50 mg in 10 mL DMSO) was again added to the mixture, and the entire process was repeated. The final precipitate was eventually dispersed in 50 mL H_2O.

To prepare Mn-MNPs for clustering and silica overcoating, we rendered the particles soluble in ethanol using PVP polymer treatment. DMSA-coated Mn-MNPs (34.7 mL, 20 mg/mL in H_2O) were mixed with PVP solution (0.65 mL, 25.6 mg/mL in H_2O), and the mixture was stirred for 1 day at room temperature. The PVP-stabilized Mn-MNPs were subsequently separated by adding aqueous acetone (H_2O/acetone = 1/10, v/v) and by centrifuging at 3220 × g for 10 minutes. The supernatant was removed, and the precipitated particles were dispersed in ethanol (10 mL). To make partially-aggregated particles, PVP treated Mn-MNPs (100 mg) were dispersed in the ethanol mixture (10 mL) with acetone (1 mL). A mixture containing a fluorescent dye (VT680), modified with APS and TEOS (TEOS/VT680 molar ratio = 0.3/0.04), was then injected into the solution of partially-aggregated particles. Polymerization was subsequently initiated by adding ammonia solution (0.86 mL, 30 wt% by NH_3), which catalyzed the production of silica-coated, multicore particles (NMPs) containing the organic dye (VT680). NMPs

(370 mg) were harvested by centrifugation (65200 × g, 30 minutes) and redispersed in basic ethanol (50 mL ; pH ~ 12). The particles were then mixed with Si-PEG (275 mg, 0.5 mmol) and APS (22 mg, 0.1 mmol), and the mixture was stirred for 2 hours at room temperature under N_2 atmosphere. The resulting NMPs were isolated from unreacted Si compounds by repeated the centrifugation (34000 × g, 20 minutes) and washing (ethanol) steps. Finally, the primary amine-terminated NMPs were dispersed in 20 mL H_2O.

Biotin or antibody conjugation: To conjugate NMPs with biotin 3-sulfo-N-hydroxysuccinimide ester sodium salt (Aldrich, Biotin-NHS, 90 %), amide bonds were formed from the primary amine on NMP via EDC chemistry. To do this, NH_2 terminated NMPs (25 mg) were dispersed in 20 mL H_2O, to which EDC (5 mg) was added. The mixture was then stirred for 3 hours at room temperature. The conjugated nanoparticles were precipitated down (30000 × g, 20 minutes) and washed three times with H_2O. To conjugate the antibodies, amine-functionalized NMPs were reacted with tetrazine through the formation of amide bonds. Briefly, 2,5-dioxopyrrolidin-1-yl 5- (4-(1,2,4,5-tetrazin-3-yl)benzylamino)-5-oxopentanoate (tetrazine-NHS) was added in excess relative to amino-NMPs, and the reaction was proceeded in PBS containing 0.1M sodium bicarbonate for 3 hours at room temperature. Following conjugation, excess tetrazine-NHS was removed through repeated centrifugation. Antibodies modified with norborene were also prepared for bioorthogonal reactions. Anti-HER2 antibodies (Herceptin, 6 mg/mL) were dissolved in 1 mL phosphate buffered saline (PBS) and adjusted to pH 8.2 by adding 0.1 M $NaHCO_3$. 2 mg succinimidyl ester of (1S,2S,4S)-bicyclo[2.2.1]hept-5-en-2-yl acetic acid was then added, and the mixture incubated for 30 minutes at 37 ^oC. The norborene-active antibodies were purified using the PD-10 desalting column (GE Healthcare Bio-Sciences) and immediately combined with the tetrazine treated NMPs (5 mg/mL). The mixture was then shaken for 6 hours at 4 ^oC and subsequently purified through centrifugation. The number of antibodies per nanoparticle was ~100, as determined by the bicinchoninic acid assay (BCA protein assay kit, Pierce Biotechnology).

***Cytotoxicity assay*.** A 3-(4,5-dimethylthiazol-2-yl)-2,5-diphenyltetrazolium (MTT) assay kit (Sigma-Aldrich) was used to evaluate cell viability in the presence of NMPs. Mouse NIH/3T3 fibroblasts were cultured in DMEM culture medium, supplemented with fetal bovine serum (FBS, 10%), penicillin and streptomycin (1%), L-glutamine (1%) and $NaHCO_3$ (2%). Human HCT116 colorectal cancer cells were cultured in vendor-provided media. Cells were maintained at 37 °C in a humidified atmosphere containing 5% CO_2. At confluence, the cells were washed, trypsinized and resuspended in culture media. Cells were then seeded at a concentration of 5,000 cells/well in a 96-well tissue culture plate and allowed to grow overnight at 37 °C under 5% CO_2. Aqueous NMP solutions at different particle concentrations were added to the culture media, and the cells were allowed to grow for a further 24 hours. Fluorescence microscopy showed the internalization of particles by treated cells. To test for cell viability, the culture media was replaced with MTT solution. After 3 hours of incubation at 37 °C under 5% CO_2, MTT solubilization solution was added to dissolve the resulting formazan crystal. Spectrophotometric measurements were obtained at a wavelength of 570 nm, with a background absorbance at 690 nm, to determine cell viability.

Avidin titration. Avidin (ImmunoPure Avidin #21121; Pierce Biotechnology) was first dissolved in PBS. The concentration of MNPs (16 nm Mn-MNPs, NMPs) was then varied to adjust T_2 to approximately 150 msec. Samples were subsequently prepared by adding 100 μL of avidin solution, containing varying avidin doses, into the prepared MNP solutions (100 μL). Control samples were likewise prepared by adding PBS (100 μL) but without avidin to the MNP solutions (100 μL); this caused T_2 to reach approximately 300 msec. After 15 minutes of incubation at 37 °C, the T_2 values of all samples were measured from 1 μL aliquots using a miniaturized nuclear magnetic resonance (NMR) system.[1-3] Carr-Purcell-Meiboom-Gill pulse sequences were used with the following parameters: echo time (TE), 4 msec; repetition time (TR), 6 sec; the number of 180° pulses per scan, 500; the number of scans, 8. We calculated ΔT_2 using the T_2 values from the control samples as a reference.

Avidin concentrations yielding $\Delta T_2 \approx 5\%$ were determined as the detection limits. All measurements were done in triplicate and data were displayed as mean ± standard error.

Cellular assay. Human SkBr3 breast cancer cells were cultured in vendor-recommended media and maintained at 37 °C in a humidified atmosphere of 5% CO_2 in air. At confluence, the cells were incubated with NMPs conjugated with HER2/*neu* antibodies for 10 minutes at 37 °C. Control samples were prepared in the same way but used NMPs without antibodies. All samples were triple-washed via centrifugation (200 × g, 5 minutes), resuspended in PBS, and serially diluted. The cell concentration of each sample was determined using a hemocytometer. T_2 measurements were obtained using the miniaturized NMR system and pulse sequences described above. ΔT_2 was calculated as the T_2 difference between targeted and control samples (cell-number matched). Cell numbers for $\Delta T_2 \approx 5\%$ were used as the detection limits. All measurements were made in triplicate and data were displayed as mean ± standard error.

Magnetic resonance imaging (MRI). Imaging was performed using a 7.0 T scanner (Bruker) and a volume coil in birdcage design (Rapid Biomedical, Germany). For phantom imaging, MNPs with different metal concentrations were prepared, and T_2 values were measured using the following spin echo parameters: TE = 10 msec; TR = 2000 msec; matrix 256 × 256; number of 180° pulses per scan = 16. For mouse imaging, NMPs conjugated with VT680 were injected intravenously with a metal dose of 10 mg [metal]/kg via tail vein. To enable co-registration with fluorescence-mediated tomography (FMT), the animal was restrained in a dedicated multimodal imaging cassette (dimensions 50 × 30 × 280 mm; VisEn Medical).[4] Images were taken while the animal was anesthetized under isoflurane (5% induction, 1.5% maintenance). T_2-weighted images were obtained using the following parameters: TE = 36 msec; TR = 2420 msec; flip angle 90°; matrix 128 × 128; field of view 4 × 4 cm^2, slice thickness 1 mm. Mice were housed and maintained under aseptic conditions according to guidelines set by the Institutional Animal Care and Use Committee.

Fluorescence-mediated tomography (FMT) imaging. Immediately after MRI, the animal (restrained in the imaging cassette) was imaged using an FMT system (FMT-2500; VisEn Medical) containing three optical channels (excitation/emission wavelengths: 635/655 nm, 680/700 nm, and 750/ 780 nm). The animal was anesthetized as for MRI. Thirty frontal slices of 0.5 mm thickness in the z direction were obtained, with an in-plane resolution of 1 × 1 mm. Following image acquisition, to calculate fluorochrome concentration, datasets were processed using a normalized Born forward equation, as previously described.[5,6]

SUPPORTING NOTE - TRANSVERSE RELAXATION MODEL

Symbols used in the text.

	Description	Unit		Description	Unit
$\Delta\omega_r$	difference of Larmor frequency	sec^{-1}	N_{mole}	number of metal atoms in a MNP	mol
τ_D	diffusion time of water	sec	C	particle concentration	counts/L
τ_{CP}	half echo time	sec	r_2^p	relaxivity per particle	$sec^{-1}\cdot L^{-1}$
D	diffusion constant of water*	cm^2/sec	r_2^m	relaxivity per metal concentration	$sec^{-1}\cdot mM^{-1}$
v	volume fraction of particles		A	lattice parameter	cm
η	sphere packing ratio		r	particle radius	cm
N_0	Avogadro constant	mol^{-1}	r_c	radius of a single MNP	cm
Z	Z factor		a_c	radius of a cluster of MNPs	cm
R_2	relaxation rate	sec^{-1}	a	overall radius of a particle	cm
μ	magnetic moments	emu	t	shell thickness	cm
M_s	Saturation magnetization	emu/cm^3	V_p	particle volume	cm^3
γ	gyromagnetic ratio	$sec^{-1}\,G^{-1}$			

* $D = 2.0 \times 10^5$ cm^2/s at 25 °C was used.[7]

1. CHEMICAL EXCHANGE (CE) MODEL

According to the chemical exchange model, relaxation rate ($R_2 = 1/T_2$) can be calculated from the following[8,9]

$$R_2 = \frac{4}{9} v \tau_D \Delta\omega_r^2 \cdot \left\{ 1 + \left(\frac{4}{9}\right)^2 \left(\frac{\tau_D}{\tau_{CP}}\right)^2 \alpha^5 \right\}^{-1}, \tag{1}$$

where

$$\alpha = \left(\frac{\Delta\omega_r \tau_{CP}}{1.34 + \Delta\omega_r \tau_{CP} v} \right)^{1/3}. \tag{2}$$

In a typical experimental condition with MNPs, in which $\Delta\omega_r \sim 10^7$ sec^{-1}, $\tau_{CP} \sim 10^{-3}$ sec, and $v \sim 10^{-5}$. T_2 is estimated at ~ 100 msec. Since $\Delta\omega_r \tau_{CP} v < 1$, α can be approximated as

$$\alpha = \left(\frac{\Delta\omega_r \tau_{CP}}{1.34} \right)^{1/3} \tag{3}$$

and Eq. (1) becomes

$$R_2 = \frac{4}{9} v \tau_D \Delta\omega_r^2 \cdot \left\{ 1 + \left(\frac{4}{9}\right)^2 \left(\frac{\tau_D}{\tau_{CP}}\right)^2 \left(\frac{\Delta\omega \tau_{CP}}{1.34}\right)^{\frac{5}{3}} \right\}^{-1}. \tag{4}$$

The volume fraction v is given as

$$v = V_p \cdot \frac{C}{1000}, \tag{5}$$

where 1000 is introduced in the denominator to convert the unit of C from [counts/L] to [counts/cm^3]. The transverse relaxivity per particle is then

$$r_2^p = R_2 / C = \frac{V_p}{1000} \cdot \frac{4}{9} \cdot \tau_D \Delta\omega_r^2 \cdot \left\{ 1 + \left(\frac{4}{9}\right)^2 \left(\frac{\tau_D}{\tau_{CP}}\right)^2 \left(\frac{\Delta\omega \tau_{CP}}{1.34}\right)^{\frac{5}{3}} \right\}^{-1}. \tag{6}$$

By defining N_{mole} as the mole-number of metal atoms in a single MNP, the transverse relaxivity per metal concentration can be obtained as follows

$$r_2^m = \frac{r_2^p}{1000 N_{mole}} = \frac{1}{1000 N_{mole}} \cdot \frac{V_p}{1000} \cdot \frac{4}{9} \cdot \tau_D \Delta\omega_r^2 \cdot \left\{ 1 + \left(\frac{4}{9}\right)^2 \left(\frac{\tau_D}{\tau_{CP}}\right)^2 \left(\frac{\Delta\omega \tau_{CP}}{1.34}\right)^{\frac{5}{3}} \right\}^{-1}. \tag{7}$$

Note that to express the relaxivity in units of [s^{-1}•mM^{-1}], another factor of 1/1000 is included.

1.1. CE model for single core MNPs

For a single core MNP with a core radius r_c and a shell thickness t, we can assume the following

$$\tau_D = a^2 / D \tag{8}$$

$$V_p = \frac{4\pi}{3} a^3 \tag{9}$$

$$\Delta\omega_r = \frac{2}{\sqrt{5}} \gamma \frac{4\pi}{3} M_s \left(\frac{r_c}{a}\right)^3 \tag{10}$$

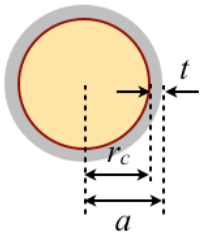

where $a = r_c + t$. The number of metal atoms in ferrite MNPs is given by

$$N_{mole} = \frac{4\pi}{3} r_c^3 \frac{3Z}{A^3 N_0}. \tag{11}$$

The r_2 relaxivity can then be obtained by substituting Eqs. (8) to (11) into Eq. (7).

1.2. CE model for NMPs.

Consider a NMP particle containing a cluster of MNPs, each with a radius r_c, and a shell of thickness t. The radii of the MNP cluster and of the NMP are a_c and a respectively. The expressions for τ_D and V_p are the same as for the single core MNPs and are given in Eqs. (8) and (9). Assuming a close-sphere stacking, the number of MNPs in a single NMP can thus be approximated as

$$\mu = N_c \left(\frac{4\pi}{3} r_c^3\right) M_s = \frac{4\pi}{3} a_c^3 \eta M_s \tag{13}$$

$$N_c = \left(\frac{a_c}{r_c}\right)^3 \eta \tag{12}$$

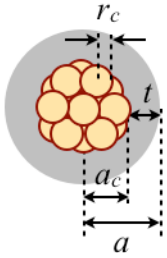

and the total magnetic moments for a NMP would be

Thus, the change in precession frequency is

$$\Delta\omega_r = \frac{2}{\sqrt{5}}\gamma\frac{4\pi}{3}M_s\eta\left(\frac{a_c}{a}\right)^3. \tag{14}$$

When the cluster is composed of ferrite particles, the total number of metal atoms can be obtained by multiplying Eq. (11) with Eq. (12)

$$N_{mole} = N_c\frac{4\pi}{3}r_c^3\cdot\frac{3Z}{A^3N_0} = \eta\frac{4\pi}{3}a_c^3\cdot\frac{3Z}{A^3N_0}. \tag{15}$$

The r_2 relaxivity is again obtained by substituting Eqs. (8), (9), (14) and (15) into Eq. (7).

2. STATIC DEPHASING (SD) MODEL

In the static dephasing regime, the relaxation rate is given by[10]

$$R_2 = \frac{\pi\sqrt{15}}{9}\nu\Delta\omega_r, \tag{16}$$

and the relaxivities per particle and per metal concentration are calculated in the same way as for the CE model

$$r_2^p = R_2 / C = \frac{V_p}{1000}\cdot\frac{\pi\sqrt{15}}{9}\Delta\omega_r, \tag{17}$$

$$r_2^m = \frac{r_2^p}{1000N_{mole}} = \frac{1}{1000N_{mole}}\cdot\frac{V_p}{1000}\cdot\frac{\pi\sqrt{15}}{9}\Delta\omega_r, \tag{18}$$

2.1. SD model for single core MNPs

Substituting Eqs. (10) and (11) into Eq. (18), we obtain

$$r_2^m = \frac{8\pi^2\sqrt{3}}{81}\cdot\frac{A^3N_0}{10^6Z}\cdot\gamma M_s. \tag{19}$$

In the SD regime, the relaxivity is independent of the particle size. For Mn-doped ferrite MNPs with r_c = 8 nm, the measured values for M_s, Z and A are 377 emu/cm^3, 8 and 8.4 Å, respectively. Thus, the estimated value for r_2^m is 759 s^{-1}mM^{-1} [metal].

2.2. SD model for NMPs

We can use Eqs. (14) and (15) to obtain an expression for r_2^m

$$\begin{aligned} r_2^m &= \frac{\pi\sqrt{15}}{9\cdot10^6}\cdot\frac{\frac{4\pi}{3}a^3}{\eta\frac{4\pi}{3}a_c^3\cdot\frac{3Z}{A^3N_0}}\cdot\frac{2}{\sqrt{5}}\gamma\frac{4\pi}{3}M_s\eta\left(\frac{a_c}{a}\right)^3 \\ &= \frac{8\pi^2\sqrt{3}}{81}\cdot\frac{A^3N_0}{10^6Z}\cdot\gamma M_s. \end{aligned} \tag{20}$$

Note that the relaxivity in the SD regime is the same for both single-core and multicore particles, and is solely dependent on the magnetization of the constituting material.

3. GLOBAL R2 MODEL

The overall r_2 behavior for various sized MNPs can be obtained by combining the results from both the CE and SD models. On the right is an example of the r_2 curves for Mn-doped ferrite MNPs (Mn-MNPs) and NMPs (containing a cluster of Mn-MNPs). For the Mn-MNPs, the particle radius (a) was allowed to grow; for NMPs, the cluster radius (a_c) was fixed to 34 nm (as is the case for real NMPs), while the shell thickness (t) was increased ($a = a_c + t$). We can summarize our observations as follows:

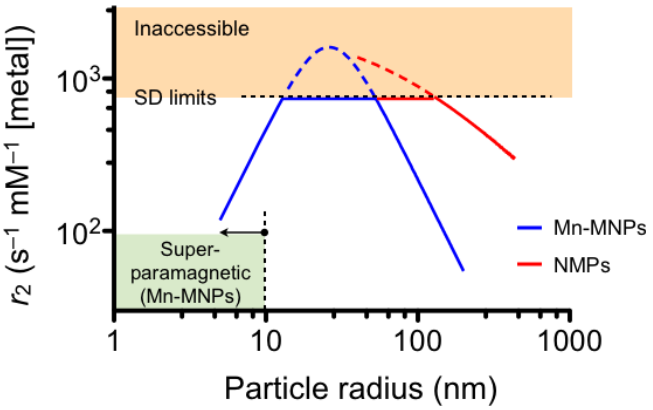

- For both Mn-MNPs and NMPs, the SD model imposes the absolute limit for r_2 growth.
- For a single-core particle (e.g., Mn-MNP) to enter the SD region, the core radius needs to be > 13 nm; this is hard to achieve in practice. Such particles are difficult to synthesize,[1] and will spontaneously aggregate in solution due to their permanent magnetic moments (i.e. they are non-superparamagnetic).
- Due to their large size, NMPs already fall within the SD region. Indeed, the construct provides a facile approach for entry into the SD regime.
- For a given material (e.g., $MnFe_2O_4$), the maximum r_2 (per metal concentration) is set solely by the magnetization, and is independent of the particle core format (i.e. single core *vs.* multicore). However, the multicore construct (e.g., NMP) appears to be the only practical approach for reaching maximum r_2.
- For large particles (a > 60 nm for Mn-MNPs; a > 150 nm for NMPs), the r_2 values decrease as they enter the so-called "Luz-Meiboom" regime.[8] Water protons that are close to the particles would not contribute to the NMR signal; their motion is completely dephased by the strong magnetic field from the particles, and cannot be restored by the spin echo sequences. Only the water protons away from the particles will contribute to the signal, therefore effectively diminishing the influence of MNPs.

REFERENCES

[1] H. Lee, T. Yoon, J. Figueiredo, F. Swirski, R. Weissleder, *Proc. Natl. Acad. Sci. USA* **2009**, *106*, 12459.
[2] D. Issadore, C. Min, M. Liong, J. Chung, R. Weissleder, H. Lee, *Lab Chip* **2011**, *11*, 2282.
[3] H. Lee, E. Sun, D. Ham, R. Weissleder, *Nat. Med.* **2008**, *14*, 869.
[4] M. Nahrendorf *et al., Proc. Natl. Acad. Sci. USA* **2010**, *107*, 7910.
[5] V. Ntziachristos, C. Tung, C. Bremer, R. Weissleder, *Nat. Med.* **2002**, *8*, 757.
[6] V. Ntziachristos, R. Weissleder, *Opt. Lett.* **2001**, *26*, 893.
[7] H. Carr, E. Purcell, Phys. Rev. **1954**, *94*, 630.
[8] R. Brooks, *Magn. Reson. Med.* **2002**, *47*, 388.
[9] P. Gillis, F. Moiny, R. Brooks, *Magn. Reson. Med.* **2002**, *47*, 257.
[10] D. Yablonskiy, E. Haacke, *Magn. Reson. Med.* **1994**, *32*, 749.